International Journal of Minerals, Metallurgy and Materials
Volume 20, Number 5, May 2013, Page 479
DOI: 10.1007/s12613-013-0754-z

Characterization and optimization of pulse electrodeposition of Ni/nano-Al_2O_3 composite coatings

A. Jegan and R. Venkatesan

Department of Mechanical Engineering, Sona College of Technology, Salem-636005, India

(Received: 26 July 2012; revised: 23 August 2012; accepted: 21 September 2012)

Abstract: Nickel/nano-Al_2O_3 composite coatings produced by the pulse electrodeposition method and the influence of pulse parameters, i.e., pulse frequency, duty cycle, and current density on the microstructure, hardness, and corrosion resistance, were critically investigated on an AISI 1018 mild steel specimen electroplated in a Watt's type bath. The experiments were carried out with different combinations of pulse parameters using Taguchi's L_{27} orthogonal array, and 27 trials were conducted to study the effect of pulse parameters in view to maximize the hardness of the specimen. The assessment results clearly reveal that the specimen exhibits the maximum hardness at the pulse frequency of 20 Hz, duty cycle of 30%, and peak current density of 0.4 A/cm^2, which are designated as the optimal parameters herein. Furthermore, the influences of those optimized pulse parameters over the microstructure and corrosion resistance were investigated, and some conclusions were drawn. Also, from the ANOVA examination, it is clear that duty cycle is predominant in affecting the hardness, while current density has relatively low impact.

Keywords: composite coatings; nickel; alumina; nanoparticles; electrodeposition; corrosion resistance; hardness

1. Introduction

Development of materials for high performance and unique characteristics has shown a drastic change after the advent of nano-technology. Synthesis of nano-structured materials has been advanced and a lot of research is being done in developing various methods for producing nano-crystalline materials for their potential properties especially strength, ductility, and corrosion resistance [1]. Ceramic particles of Al_2O_3 coatings have various applications, such as gas bearings, electrical insulation, and thin film structures of magnetic heads for tape and disc drives, and they exhibit high hardness, melting point, and extreme chemical stability [2]. Ni/Al_2O_3 coatings are highly abrasive and heat resistant and have relatively good anti-corrosion properties. They can be attractive alternatives, particularly to chromium coatings [3]. Electro-deposition of pulse plating is a very versatile method, which can yield nano-crystalline coatings with improved surface appearance and properties, such as smoothness, refined grains, and enhanced corrosion resistance [4-5]. Electroplating is simple in operation and can be controlled precisely near room temperature. It has low-energy requirement and the capability of coating components with complex geometrics; the thickness of plating layer can be controlled by adjusting current density and electroplating time [6-7]. Pulse plating can give a homogenous distribution of particles, reduce waste, serve to control the microstructure composition of the coatings, and has the capability of continuous processing [8-9]. The structure and properties of composite coatings depend not only on the concentration, size, distribution, and nature of the reinforced particles but also on the type of solution used and electroplating parameters (frequency, duty cycle, current density, temperature, and pH value) [10]. Pulse plating parameters, such as low pulse frequency, duty cycle, and current densities, give more hardness, less wear, and corrosion resistance [11-13]. Baboian [14] stated that the Salt Spray test, when used properly, is one of the most valuable corrosion tests in the world. It has impacted industries in all sectors. It has been very valuable in terms of quality control and comparative behavior materials and that is in all walks of life: in automotive, aircraft, and compliance industries and

Corresponding author: A. Jegan E-mail: jegmak@gmail.com
© University of Science and Technology Beijing and Springer-Verlag Berlin Heidelberg 2013

in transportation and infrastructure. Taguchi techniques for quality engineering can give better optimum results [15-16]. Moreover, Hou and Chen [9] used the Taguchi technique for the optimization of pulse parameters. However, to the authors' knowledge, only negligible quantum of work has been carried out in optimizing pulse parameters for maximizing the hardness. This research work mainly focuses on the pulse parameter optimization of Ni/nano-Al_2O_3 composites using a mild steel specimen by Taguchi's L27 orthogonal array concept, and thereby determining the optimum values which will maximize the hardness value. Furthermore, the corresponding microstructure and corrosion resistance of the specimen were also investigated.

2. Experimental procedures

A typical Watts-type bath was prepared for the electrodeposition process. The composition and the experimental parameters are shown in Table 1. The Al_2O_3 particles in sizes varying from 40 to 50 nm were used in the experiment. Before the codeposition process, the suspended solution was stirred for 6 h, and then, ultrasonic vibration was executed for 30 min. The pH value of the bath was adjusted with nickel carbonate (25wt%) and sulphuric acid (25wt%) solution, and a distinctive value of 4 was maintained throughout the experiment. AISI 1018 mild steel plates of 10 mm in diameter and 32 mm in length on both sides were used as the cathode; the surface length of the substrate was blocked with a polyvinyl chloride (PVC) adhesive tape; and the anode was made of a pure Ni plate. The samples were metallographically prepared, immersed in acetone, and then kept in an ultrasonic stirrer for 5 min. This was done to clean the sample for impurities. The substrates were then immersed in the bath using holding devices. They were activated in a mixed acidic bath at room temperature before electroplating. Substrates were placed parallel to a vertically oriented nickel plate at a distance of 5 cm in the above-mentioned bath. A Dynatronix (USA) pulse rectifier was used to supply pulse current at various frequencies, duty cycles, and current densities. During the codeposition process, the bath was stirred at a rate of 550 r/min by a magnetic stirrer to keep the particles dispersed and prevent sedimentation in the electrolyte suspension. After depositing the coating, the thickness was found using a metallurgical microscope, Metscope-1. The crystal structure of the composite coatings was studied by X-ray diffraction (SEIFERT), and the surface morphology of the coatings was observed using a Quanta-200 scanning electron microscope (SEM). The percentage of codeposited Al_2O_3 particles was evaluated by using energy dispersive X-ray spectroscopy (EDX). Hardness of the coatings was determined using a Vickers micro hardness Shimadzu tester (HMV 2T indenter) with a load of 0.49 N for 15 s. The same trial was repeated for ten times, and the average value was quoted as the final hardness. The corrosion salt spray test following ASTM B117-07 standards was conducted over the optimized specimen in the following conditions: NaCl concentration, 5wt%±0.1wt%; camper temperature, 33.8-34.8°C; pH 6.7; air pressure, 103421 Pa; and the collection of solution, 1.3-1.4 mL/h. The specimen was gently cleaned and dried immediately before and after the test.

Table 1. Basic bath compositions and electrodeposition conditions

Concentration of $NiSO_4 \cdot 6H_2O$ / ($g \cdot L^{-1}$)	330
Concentration of $NiCl_2 \cdot 6H_2O$ / ($g \cdot L^{-1}$)	50
Concentration of Sodium dodecyl sulfate / ($g \cdot L^{-1}$)	0.1
Concentration of Al_2O_3 particle / ($g \cdot L^{-1}$)	40
Temperature / °C	60±2
pH value	4
Pulse frequency / Hz	10, 20, 30
Pulse duty cycle / %	10, 20, 30
Pulse current density / ($A \cdot cm^{-2}$)	0.2, 0.4, 0.6

2.1. Pulse computation

The following equations are used to compute the values of duty cycle, frequency, total time, average current, and peak current.

$$\text{Duty cycle} = T_{\text{ON}} / (T_{\text{ON}} + T_{\text{OFF}}) \tag{1}$$

$$\text{Frequency} = 1/\text{Total time} \tag{2}$$

$$\text{Total time} = T_{\text{ON}} + T_{\text{OFF}} \tag{3}$$

$$I_{\text{A}} = I_{\text{p}} \times \text{ Duty cycle} \tag{4}$$

$$I_{\text{P}} = \text{Peak pulse current / Surface area} \tag{5}$$

where T_{ON} is the on-time, T_{OFF} the off-time, I_{A} the average pulse current density, and I_{P} the peak current density.

2.2. Plan of experiments (Taguchi's techniques)

Experiments were conducted based on the Taguchi's method at three levels, each with three factors. The values taken by a factor are termed to be levels. The factors to be studied and their levels chosen are detailed in Table 2.

Table 2. Factors and levels

Factor	Level		
	1	2	3
Frequency / Hz	10	20	30
Duty cycle / %	10	20	30
Current density / ($A \cdot cm^{-2}$)	0.2	0.4	0.6

2.3. Signal-to-noise ratio (S/N ratio)

The S/N ratio for micro hardness is calculated using the-higher-the-better criterion, which was given by Taguchi [17], as depicted in Eq. (6):

$$\text{S/N} = -\ 10 \lg \left(\frac{1}{n} \cdot \sum \frac{1}{y^2} \right) \tag{6}$$

where y is the observed data and n is the number of observations. From the orthogonal array used, it is possible to get the effects of each factor at different levels. For instance, the average S/N ratio for factor A at levels 1, 2, and 3 can be obtained by calculating the mean of S/N ratios for trials 1-9, 10-18, and 19-27, respectively. The mean S/N ratio for each level of all other factors is computed in similar fashion. Here, the L_{27} orthogonal array is used for experimental investigations.

The 27 experimental microhardness results are tabulated, and the corresponding mean S/N ratio results are calculated by considering the method that choosing higher is better. Table 3 clearly shows the optimum level of the experiment, i.e., the maximum hardness at frequency 20 Hz, duty cycle 30%, and peak current density 0.4 A/cm^2. The results of ANOVA for the Ni/nano-Al_2O_3 composite coatings under different pulse parameters, such as frequency, duty cycle, and current density, are shown in Table 4. From the ANOVA results, duty cycle seems to be predominant in affecting hardness (54.59%). The percentage of error for this experiment is obtained within the optimum level. The results of percentage contribution and the main effect of Ni/nano-Al_2O_3 composite coatings are represented in Figs. 1 and 2, respectively. The graph is drawn to levels versus the mean S/N ratio for microhardness. Each level

Table 3. Experimental results for microhardness and S/N ratio

Exp. No.	Frequency / Hz	Duty cycle / %	Current density / (A · cm^{-2})	Surface area (SA) / cm^2	Peak current / A	Average current / A	T_{on} / ms	T_{off} / ms	Plating time / min	Hv	S/N ratio
1	10	10	0.2	1.57	0.314	0.031	10	90	11.506	154.8	53.80
2	10	10	0.4	1.57	0.628	0.062	10	90	11.506	141.1	52.99
3	10	10	0.6	1.57	0.942	0.094	10	90	11.506	142.0	53.05
4	10	20	0.2	1.57	0.314	0.062	5	45	11.506	166.5	54.43
5	10	20	0.4	1.57	0.628	0.125	5	45	11.506	201.4	56.08
6	10	20	0.6	1.57	0.942	0.188	5	45	11.506	158.6	54.01
7	10	30	0.2	1.57	0.314	0.094	3.33	30	11.506	190.2	55.58
8	10	30	0.4	1.57	0.628	0.188	3.33	30	11.506	200.6	56.05
9	10	30	0.6	1.57	0.942	0.282	3.33	30	11.506	203.0	56.15
10	20	10	0.2	1.57	0.314	0.031	20	80	11.506	159.2	54.04
11	20	10	0.4	1.57	0.628	0.062	20	80	11.506	182.1	55.21
12	20	10	0.6	1.57	0.942	0.094	20	80	11.506	170.6	54.64
13	20	20	0.2	1.57	0.314	0.062	10	40	11.506	185.0	55.34
14	20	20	0.4	1.57	0.628	0.125	10	40	11.506	205.0	56.24
15	20	20	0.6	1.57	0.942	0.188	10	40	11.506	201.6	56.09
16	20	30	0.2	1.57	0.314	0.094	6.66	26.66	11.506	215.5	56.67
17	20	30	0.4	1.57	0.628	0.188	6.66	26.66	11.506	262.9	58.40
18	20	30	0.6	1.57	0.942	0.282	6.66	26.66	11.506	236.3	57.47
19	30	10	0.2	1.57	0.314	0.031	30	70	11.506	160.3	54.10
20	30	10	0.4	1.57	0.628	0.062	30	70	11.506	162.0	54.19
21	30	10	0.6	1.57	0.942	0.094	30	70	11.506	151.8	53.63
22	30	20	0.2	1.57	0.314	0.062	15	35	11.506	167.8	54.50
23	30	20	0.4	1.57	0.628	0.125	15	35	11.506	207.6	56.34
24	30	20	0.6	1.57	0.942	0.188	15	35	11.506	180.0	55.11
25	30	30	0.2	1.57	0.314	0.094	10	23.33	11.506	179.5	55.08
26	30	30	0.4	1.57	0.628	0.188	10	23.33	11.506	220.4	56.86
27	30	30	0.6	1.57	0.942	0.282	10	23.33	11.506	171.5	54.69

Table 4. ANOVA results for the microhardness of Ni/nano-Al_2O_3 composite coatings

Source of variance	Degree of freedom	Sum of squares	Mean sum of squares (variance)	F ratio	Contribution / %
Frequency	2	8.91	4.46	12.30	19.09
Duty cycle	2	25.49	12.75	35.18	54.59
Current density	2	5.05	2.52	6.96	10.81
Error	20	7.25	0.36	—	15.52
Total	26	46.70	—	—	100

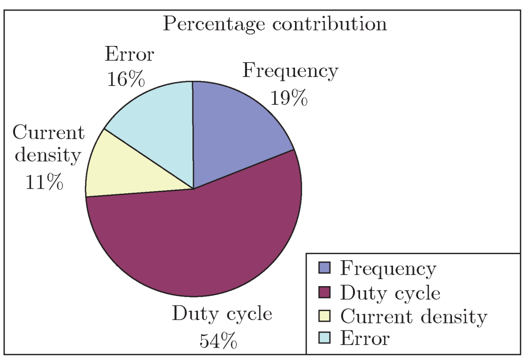

Fig. 1. Percentage contribution of the pulse plating parameters of Ni/nano-Al_2O_3 composite coatings.

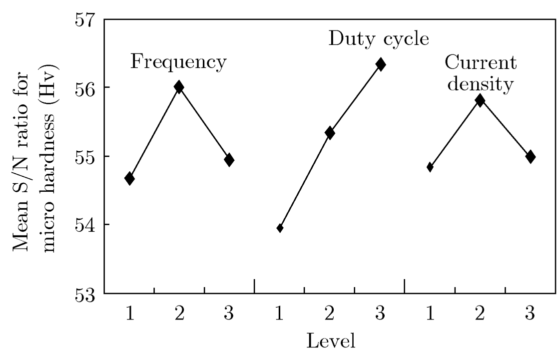

Fig. 2. Mean S/N ratio for different microhardnesses of Ni/nano-Al_2O_3 composite coatings.

has three factors and the maximum values are selected for each level. The optimum values are 2, 3, and 2, i.e., frequency 20 Hz, duty cycle 30%, and peak current density 0.4 A/cm^2.

3. Results and discussion

3.1. Surface morphology and microstructural characterization

At the optimized surface parameters having a frequency of 20 Hz, duty cycle of 30%, peak current density of 0.4 A/cm^2, the surface of a nickel/nano-Al_2O_3 composite coating was observed under a scanning electron microscope. Fig. 3 shows that the Al_2O_3 particles are homogeneous and have 'leaf shape' distribution over the entire coated surface of the nickel matrix. Whilst, most of the reported works dealing with "Ni/nano-Al_2O_3 co-deposition work" produces 'pyramidal crystal' microstructures [3-5, 8, 12, 18-19]. Moreover, the alumina particles (Figs. 3(c) and 3(d)) appear as bright spots in the dark nickel matrix. The EDX (Fig. 4) analyses were performed on the surface

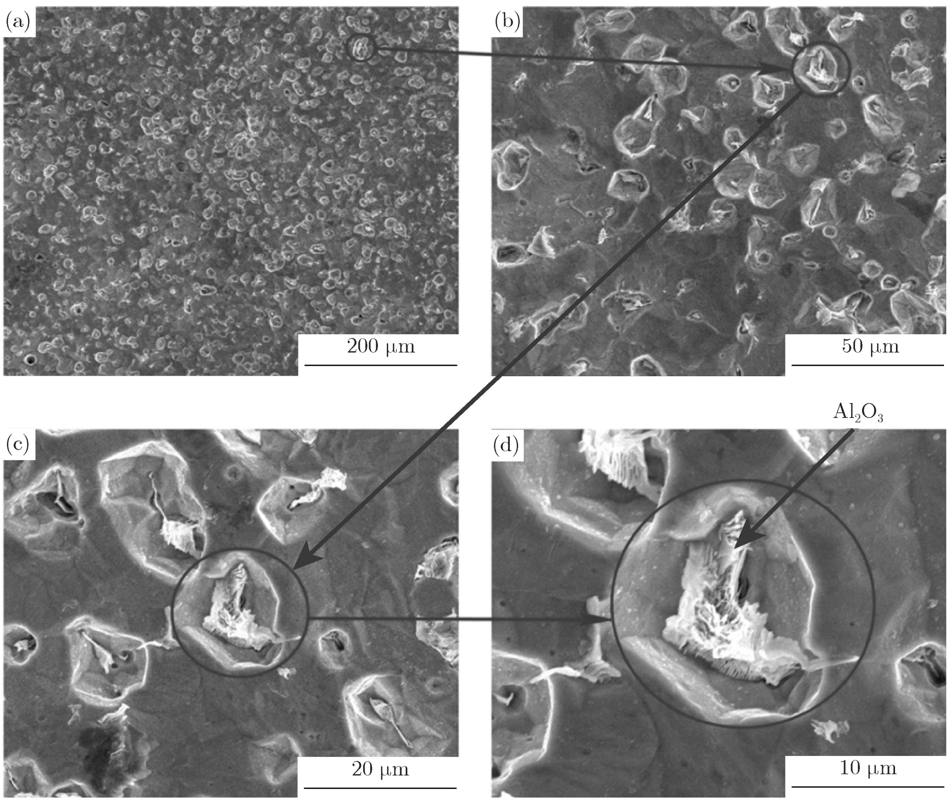

Fig. 3. SEM images of Ni/nano-Al_2O_3 composite coatings prepared at the frequency of 20 Hz, duty cycle of 30%, and peak current density of 0.4 A/cm^2.

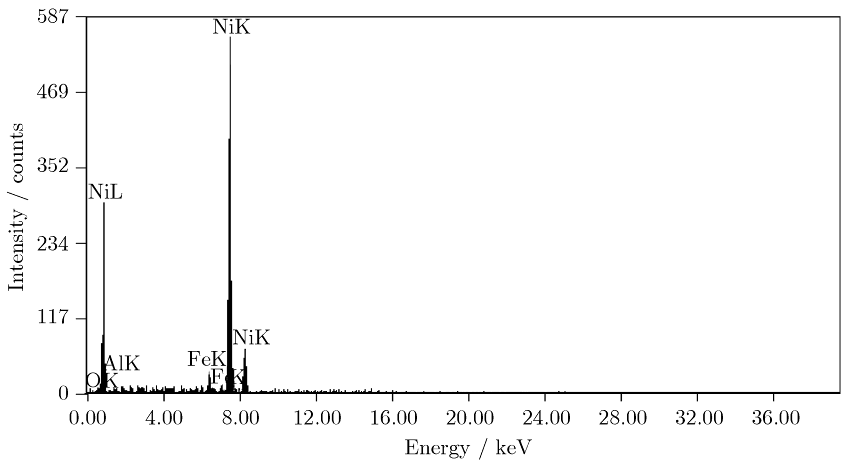

Fig. 4. EDX spectrum of the Ni/nano-Al_2O_3 composites of AISI 1018 mild steel.

of the specified single leaf shape area (Fig. 3(d)). The examinations show that the aluminum (AlK) and oxide (OK) contents are 5.29at% and 13.67at%, respectively. The analysis reveals that oxides are the dominant elements in the Ni matrix.

3.2. XRD analysis

XRD patterns of Ni/nano-Al_2O_3compositesprepared by the optimum mild steel specimen at frequency 20 Hz, duty cycle 30%, and peak current density 0.4 A/cm^2 by pulse electrodeposition methods are shown in Fig. 5. The composite coatings exhibit face-centered cubic (fcc) lattice with different orientations, which are influenced by the pulse frequency, duty cycle, and current density. It can be clearly observed that the composite coating exhibits obvious (111) preferred orientation at low pulse frequency and higher duty cycle [5, 10]. Furthermore, Jung *et al.* [5] found that the reflection intensities of (200) and (220) planes were very low, and Chen *et al.* [10] reported that the texture coefficients of the composite coatings prepared under different frequencies (10, 500, and 1000 Hz) were in the order of (111) > (200) > (311) > (220). Compared with direct current (DC) and pulse reverse current (PRC) coatings [18], the width and orientation of diffraction peaks (111), (200), and (220) of the present pulse current coatings are equal. The present investigation result shows that by means of the pulse current technique, fine-grained texture, smooth surface, and compact microstructure of the coatings can be achieved.

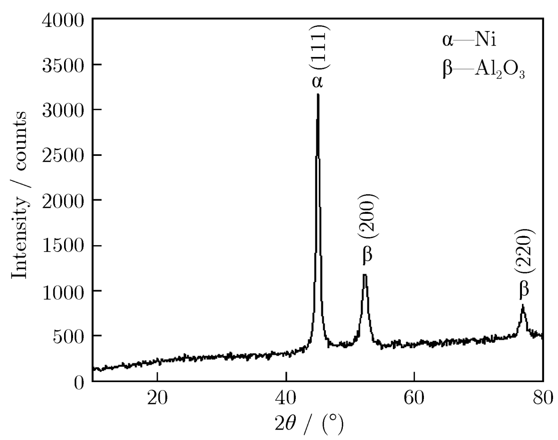

Fig. 5. XRD patterns of Ni/nanoAl_2O_3 composites prepared at the frequency of 20 Hz, duty cycle of 30%, and peak current density of 0.4 A/cm^2.

3.3. Microhardness

Microhardness measurements were performed on the surface of the pulse plated Ni/nano-Al_2O_3 coatings using Taguchi's techniques. The optimized values are found from Table 3. The reported values are obtained at frequency 20 Hz, duty cycle 30%, and peak current density 0.4 A/cm^2. Compared to DC plating, pulse plating produces harder coatings. This indicates that bath chemistry has influenced the hardness of the coating. Furthermore, the hardness and wear resistance, as well as the macro residual stress of coatings, change with the increasing content of Al_2O_3 particles in the coatings [5]. Comparing with pulse reverse coatings, the hardness (Hv 262.9) and the content of Al_2O_3 (AlK, 3.24wt%; OK, 4.97wt%) of pulse current coatings are found significantly identical. From the data, it can be observed that the nano-Al_2O_3 content and the high peak current density produced by pulse plating have influenced the microstructure of the coating which in turn influences the hardness.

3.4. Coating thickness

The coating thickness with optimized pulse parameters was investigated using METSCOPE-1, a metallurgical microscope (Fig. 6), and it was identified by the cross-section of the specimen following ASM standards. It is observed that the addition of nano-Al_2O_3 particles in the plating bath significantly decreases the coating deposit thickness at the same plating time and increases the surface roughness. It is seen obviously that the electro-deposited growing layer is a competition between nucleation and crystal growth steps. The addition of nano-Al_2O_3 particles leads to a lower deposition rate of nickel coatings. It also decreases the diffusion area of Ni^{2+} ions and provides more nucleation sites to the detriment of crystal growth. Therefore, the coating thickness (11.6 μm) decreases with the increase in amount of nano-Al_2O_3 particles in the coatings [6]. Moreover, the results produced the coating thickness of 14 μm, which is significantly identical to the results of Feng *et al.* [6].

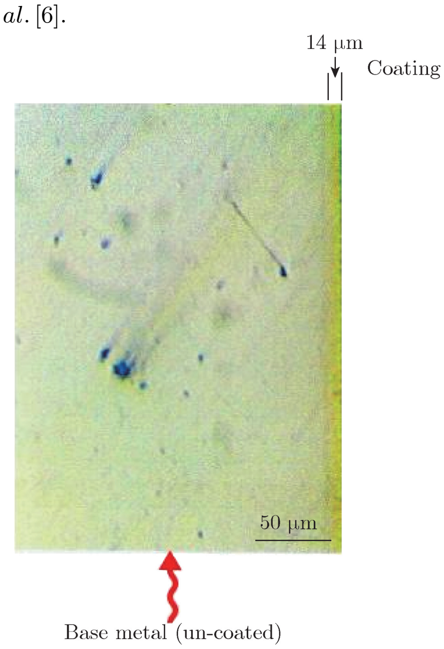

Fig. 6. Coating thickness of Ni/nano-Al_2O_3 composite coatings.

3.5. Corrosion studies

The salt spray test practice provides a controlled corrosive environment, which has been utilized to produce relative corrosion resistance information for the specimens of metals and coated metals exposed in a given test chamber [20]. The salt spray method was used to study the corrosion effects. The experimentations were carried out by satisfying ASTM B117-2007 standards. The sample was checked periodically for the first 28-35 h, and no corrosion was present in the sample. After 35 h, the sample started corroding, until it stabilized at 48 h. After 48 h, red rust appearance was found on the specimen (Fig. 7).

Fig. 7. Result of the corrosion salt spray test.

3.6. Confirmation test

The confirmation experiment is the final step in the first iteration of the design of the experiment process. The purpose of this experiment is to validate the conclusions drawn during the analysis phase. It was performed by conducting a test with a specific combination of the factors and levels previously evaluated. In this study, after identifying the optimum process parameters (frequency, 20 Hz; duty cycle, 30%; and peak current density, 0.4 A/cm^2), the settings were used again to produce a new specimen with coating, and its corresponding hardness value was evaluated. The magnitude of hardness was Hv 263.7. It is evident that the S/N ratio is improved by a value of 0.02 from the conformation test process parameter, which is an agreeable degree of approximation. It is also evident that duty cycle is predominant in deciding the hardness value.

4. Conclusions

(1) The optimum values of pulse parameters were estimated using Taguchi's technique and the hardness value was found to be maximum (Hv 262.9) under the following conditions: frequency, 20 Hz; duty cycle, 30%; and peak current density, 0.4 A/cm^2.

(2) Duty cycle is predominant (54%) in deciding the hardness of the specimen.

(3) The SEM investigation shows that the 'leaf shape' Al_2O_3 particles are compactly embedded into the Ni matrix.

(4) The EDX analysis confirms that the coating is mainly composed of Ni/Al_2O_3.

(5) A coating thickness of 14 μm was achieved and better corrosion resistance characteristics were derived.

In general, this investigation shows that the hardness of a composite coating containing ceramic particulates can be varied by changing pulse parameters, such as frequency, duty cycle, and current density without any alteration in electrodeposition conditions or the bath composition.

Acknowledgements

The authors gratefully acknowledge the support provided by the Indian Institute of Technology (IIT), Madras, the Centre for Material Joining and Research (CEMAJOR), Annamalai University Chidambaram, Tamilnadu, and the Omega Inspection and Analytical Lab., Chennai, India.

References

[1] R. Srivathsan, G. Karthick Venkatesh, R. Arunachalam, A. Jegan, and J. Prasanna Kumar, Development of nano crystalline nickel coating for engineering applications, *Key Eng. Mater.*, 443(2010), p. 487.

[2] Z.N. Farhat, Wear resistant composite coatings, *Mater. Charact.*, 60(2009), p. 337.

[3] B. Szczygie and M. Ko o dziej, Composite Ni/Al_2O_3 coatings and their corrosion resistance,. *Electrochim. Acta*, 50(2005), p. 4188.

[4] D. Thiemig, R. Lange, and A. Bund, Influence of pulse plating parameters on the electrocodeposition of matrix metal nanocomposites, *Electrochim. Acta*, 52(2007), p. 7362.

[5] A. Jung, H. Natter, R. Hempelmann, and E. Lach, Nanocrystalline alumina dispersed in nanocrystalline nickel: enhanced mechanical properties, *J. Mater. Sci.*, 44(2009), p. 2725.

[6] Q.Y. Feng, T.J. Li, Z.T. Zhang, J. Zhang, M. Liu, and J. Jin, Preparation of nanostructured Ni/Al_2O_3 composite coatings in high magnetic field, *Surf. Coat. Technol.*, 201(2007), p. 6247.

[7] R.K. Saha and T.I. Khan, Effect of applied current on the electrodeposited $Ni-Al_2O_3$ composite coatings, *Surf. Coat. Technol.*, 205(2010), p. 890.

[8] D. Thiemig, A. Bund, and J.B. Talbot, Influence of hydrodynamics and pulse plating parameters on the electrocodeposition of nickel-alumina nanocomposite films, *Electrochim. Acta*, 54(2009), p. 2491.

[9] K.H. Hou and Y.C. Chen, Preparation and wear resistance of pulse electrodeposited $Ni-W/Al_2O_3$ composite coatings, *Appl. Surf. Sci.*, 257(2011), p. 6340.

[10] L. Chen, L.P. Wang, Z.X. Zeng, and T. Xu, Influence of pulse frequency on the microstructure and wear resistance of electrodeposited Ni-Al_2O_3 composite coatings, *Surf. Coat. Technol.*, 201(2006), p. 599.

[11] M.E. Bahrololoom and R. Sani, The influence of pulse plating parameters on the hardness and wear resistance of nickel-alumina composite coatings, *Surf. Coat. Technol.*, 192(2005), p. 154.

[12] D. Thiemig and A. Bund, Influence of ethanol on the electrocodeposition of Ni/Al_2O_3 nanocomposite films, *Appl. Surf. Sci.*, 255(2009), p. 4164.

[13] L. Chen, L.P. Wang, Z.X. Zeng, and Z.Y. Zhang, Effect of surfactant on the electrodeposition and wear resistance of Ni-Al_2O_3 composite coatings, *Mater. Sci. Eng. A*, 434(2006), p. 319.

[14] R. Baboian, *Corrosion Tests and Standards: Application and Interpretation*, 2nd Ed., ASTM International, 2005.

[15] K.L. Senthil Kumar, R. Sivasubramanian, and K. Kalaiselvan, Selection of optimum parameters in non conventional machining of metal matrix composite, *Portugaliae Electrochim. Acta*, 27(2009), p. 477.

[16] B.M. Gopalsamy, B. Mondal, and S. Ghosh, Taguchi method and ANOVA: an approach for process parameters optimization of hard machining while machining hardened steel, *J. Sci. Ind. Res.*, 68(2009), p. 686.

[17] P.J. Ross, *Taguchi Techniques for Quality Engineering*, Tata McGraw Hill Publishing Co. Ltd., New Delhi, 2005.

[18] L.M. Chang, M.Z. An, and S.Y. Shi, Microstructure and characterization of Ni-Co/Al_2O_3 composite coatings by pulse reversal electrodeposit, *Mater. Chem. Phys.*, 100(2006), p. 395.

[19] X.T. Yuan, Y. Wang, D.B. Sun, and H.Y. Yu, Influence of pulse parameters on the microstructure and microhardness of nickel electrodeposits, *Surf. Coat. Technol.*, 202(2008), p. 1895.

[20] *ASTM B117-03 Standard Practice for Operating Salt Spray (Fog) Apparatus*, ASTM International, West Conshohocken, 2003.